



United States Nuclear Regulatory Commission

Protecting People and the Environment

NUREG/CR-7103, Vol. 1
PNNL-16613

Pacific Northwest National Laboratory Investigation of Stress Corrosion Cracking in Nickel-Base Alloys, Volume 1

Office of Nuclear Regulatory Research

**AVAILABILITY OF REFERENCE MATERIALS
IN NRC PUBLICATIONS**

NRC Reference Material

As of November 1999, you may electronically access NUREG-series publications and other NRC records at NRC's Public Electronic Reading Room at <http://www.nrc.gov/reading-rm.html>. Publicly released records include, to name a few, NUREG-series publications; *Federal Register* notices; applicant, licensee, and vendor documents and correspondence; NRC correspondence and internal memoranda; bulletins and information notices; inspection and investigative reports; licensee event reports; and Commission papers and their attachments.

NRC publications in the NUREG series, NRC regulations, and *Title 10, Energy*, in the Code of *Federal Regulations* may also be purchased from one of these two sources.

1. The Superintendent of Documents
U.S. Government Printing Office
Mail Stop SSOP
Washington, DC 20402-0001
Internet: bookstore.gpo.gov
Telephone: 202-512-1800
Fax: 202-512-2250
2. The National Technical Information Service
Springfield, VA 22161-0002
www.ntis.gov
1-800-553-6847 or, locally, 703-605-6000

A single copy of each NRC draft report for comment is available free, to the extent of supply, upon written request as follows:

Address: U.S. Nuclear Regulatory Commission
Office of Administration
Publications Branch
Washington, DC 20555-0001
E-mail: DISTRIBUTION.RESOURCE@NRC.GOV
Facsimile: 301-415-2289

Some publications in the NUREG series that are posted at NRC's Web site address <http://www.nrc.gov/reading-rm/doc-collections/nuregs> are updated periodically and may differ from the last printed version. Although references to material found on a Web site bear the date the material was accessed, the material available on the date cited may subsequently be removed from the site.

Non-NRC Reference Material

Documents available from public and special technical libraries include all open literature items, such as books, journal articles, and transactions, *Federal Register* notices, Federal and State legislation, and congressional reports. Such documents as theses, dissertations, foreign reports and translations, and non-NRC conference proceedings may be purchased from their sponsoring organization.

Copies of industry codes and standards used in a substantive manner in the NRC regulatory process are maintained at—

The NRC Technical Library
Two White Flint North
11545 Rockville Pike
Rockville, MD 20852-2738

These standards are available in the library for reference use by the public. Codes and standards are usually copyrighted and may be purchased from the originating organization or, if they are American National Standards, from—

American National Standards Institute
11 West 42nd Street
New York, NY 10036-8002
www.ansi.org
212-642-4900

Legally binding regulatory requirements are stated only in laws; NRC regulations; licenses, including technical specifications; or orders, not in NUREG-series publications. The views expressed in contractor-prepared publications in this series are not necessarily those of the NRC.

The NUREG series comprises (1) technical and administrative reports and books prepared by the staff (NUREG-XXXX) or agency contractors (NUREG/CR-XXXX), (2) proceedings of conferences (NUREG/CP-XXXX), (3) reports resulting from international agreements (NUREG/IA-XXXX), (4) brochures (NUREG/BR-XXXX), and (5) compilations of legal decisions and orders of the Commission and Atomic and Safety Licensing Boards and of Directors' decisions under Section 2.206 of NRC's regulations (NUREG-0750).

DISCLAIMER: This report was prepared as an account of work sponsored by an agency of the U.S. Government. Neither the U.S. Government nor any agency thereof, nor any employee, makes any warranty, expressed or implied, or assumes any legal liability or responsibility for any third party's use, or the results of such use, of any information, apparatus, product, or process disclosed in this publication, or represents that its use by such third party would not infringe privately owned rights.

Pacific Northwest National Laboratory Investigation of Stress Corrosion Cracking in Nickel-Base Alloys, Volume 1

Manuscript Completed: August 2011
Date Published: September 2011

Prepared by
S. M. Bruemmer and M. B. Toloczko

Pacific Northwest National Laboratory
P.O. Box 999
Richland, WA 99352

E. G. Reichelt, NRC Project Manager

NRC Job Code N6007

Abstract

The objective of this ongoing program is to conduct stress-corrosion cracking (SCC), crack-growth-rate (CGR) testing of nickel-base stainless alloys in high-temperature, light-water-reactor (LWR) environments. An emphasis is placed on structural alloys with higher Cr content, specifically alloy 690 and its weld metals alloy 152 and 52. Other relevant nickel- and iron-base alloys may also be in the test matrix including materials removed from LWR service. In order to accomplish this objective, autoclave systems in suitable load frames and the associated water supply, conditioning and pressurization subsystems were designed and constructed. These autoclave systems enable testing under simulated and/or accelerated pressurized-water reactor (PWR) and boiling-water reactor (BWR) conditions (e.g., increased temperature, more aggressive chemical environments, increased load range or load interaction effects) with quantitative in-situ measurement of crack extension and electrochemical corrosion potential.

Three CGR test systems have been assembled and capabilities qualified through experiments first on cold-worked (CW), 300-series, austenitic stainless steels in high-purity BWR environments followed by tests on CW alloy 600 and alloy 182 weld metal in both BWR and PWR environments as part of round-robin collaborations. The CGR tests on stainless steels evaluated stress intensity, cyclic loading, ECP, and sulfate additions on SCC propagation rates. These tests were also used to demonstrate accurate control of environmental/mechanical test conditions and reproducible direct-current, potential drop (dcpd) crack-length measurements with resolution down to micrometer dimensions.

Crack-growth responses of five CW 316SS samples were evaluated and all heats exhibited consistent intergranular stress corrosion crack propagation rates in oxidizing, high-purity BWR water. Unexpected high crack-growth rates at low ECPs in BWR hydrogen water chemistry (HWC) conditions were observed for one CW 316LSS heat. Two samples of this material were tested in different systems over a range of stress intensities and hydrogen levels showing propagation rates near 10^{-7} mm/s. Only a small decrease (2–3X) was seen at HWC in comparison to BWR oxidizing conditions (2000 ppb O_2). The other two CW 316SS heats evaluated exhibited the more typical benefit when adding H_2 and removing O_2 from the water with CGRs decreased by a factor of 50–100 times. Round-robin CGR testing (organized by the International Cooperative Group on Environment-Assisted Cracking [ICG-EAC]) was performed on alloy 600 and alloy 182 materials. Experiments were conducted in BWR oxidizing water for both alloys and in simulated PWR primary water for the alloy 182 weld metal. Results demonstrated state-of-the-art capabilities for the Pacific Northwest National Laboratory (PNNL) systems and testing methodology through comparisons with other laboratories in the U.S., Europe, and Japan. Stable and reproducible crack extension could be measured at length changes below $1 \mu\text{m}$ enabling propagation rates to be documented below 10^{-9} mm/s. In addition, the influence of H_2 content on stress corrosion in PWR primary water was examined for alloy 182 weld metal documenting higher propagation rates at intermediate H_2 concentrations where the specimen ECP crosses the Ni/NiO transition line at 325°C (617°F). Preliminary data for the first tests on alloy 152 weld metal and alloy 690 control rod drive mechanism (CRDM) materials are also described along with various characterization activities on the project materials.

Foreword

Primary water stress corrosion cracking (PWSCC) is a significant issue that has affected nickel base alloy pressurized-water reactor (PWR) components. Observation of PWSCC in the past decade has challenged the assumptions of leak before break (LBB) analyses. These analyses did not consider active degradation mechanisms such as PWSCC that may contribute to potential sources of pipe rupture, and subsequently, a loss of coolant accident (LOCA). In addition, operational experience has shown that PWSCC of reactor pressure vessel head (RPVH) penetrations can lead to boric acid corrosion of low-alloy pressure vessel steels.

The U.S. Nuclear Regulatory Commission (NRC) mandated inspections are required for reactor coolant system components constructed from PWSCC susceptible materials including alloys 600 and its weld metals, alloys 182 and 82. Because, these inspections are costly to implement and result in occupational exposures, the industry has proposed methods for PWSCC mitigation such as the use of components manufactured from alloy 690 and its weld metals alloys 152 and 52. While the operational experience of these higher chromium containing alloys has been favorable, the effects of operating conditions and metallurgical factors on PWSCC susceptibility are not fully understood. Ongoing industry-led research has been conducted to evaluate metallurgical and environmental effects that influence PWSCC resistance. Confirmatory testing sponsored by the NRC has been conducted to verify improvement factors and to support inspection intervals for components manufactured from the higher chromium containing alloys.

This report documents work conducted by Pacific Northwest National Laboratory (PNNL) during calendar years 2005 and 2006 under contract to the NRC. Testing conducted during this period consisted of assembling three crack growth rate testing systems, verification of system capability and measurement resolution, crack growth rate testing, and material characterization. Initial tests included cold worked alloy 600 and alloy 182 weld metal that were evaluated as part of round-robin testing conducted at both domestic and international laboratories. Tests were also conducted on the higher chromium containing alloy 690 control rod drive mechanism (CRDM) tubing and alloy 152 welds from industry mockups of replacement components. Results of these tests along with compositional maps and initial high resolution imaging of crack tips suggest that the higher chromium base and weld metals are more resistant to PWSCC.

Additional testing and analyses will be conducted on alloy 690. These tests will include material with expected ranges of cold work and thermal treatments. Testing also will be conducted with additional alloy 152 and 52 weld samples to determine the factors that affect PWSCC resistance in the high chromium weld alloys. The combination of microstructural and crack tip analyses on test materials with known crack growth rates will contribute to both industry-led research and support inspection criteria for existing and new reactors.

Michael J. Case, Director
Division of Engineering
Office of Nuclear Regulatory Research
U.S. Nuclear Regulatory Commission

Contents

| | |
|---|------------|
| Abstract..... | iii |
| Foreword..... | v |
| Executive Summary | xi |
| Acknowledgments..... | xiii |
| Acronyms and Abbreviations..... | xv |
| 1 Introduction | 1-1 |
| 2 Design of SCC Crack-Growth Test Systems..... | 2-1 |
| 3 Construction and Shakedown Testing of SCC Crack-Growth Systems | 3-1 |
| 3.1 Construction and Assembly Activities..... | 3-1 |
| 3.2 General SCC Crack-Growth Testing Approach | 3-6 |
| 3.3 Proof Testing for the DCPD System | 3-10 |
| 3.4 Crack Growth System Shakedown Testing | 3-14 |
| 4 Validation Testing and Round-Robin SCC Crack-Growth Rate Testing | 4-1 |
| 4.1 Cold-Worked Austenitic Stainless Steels..... | 4-1 |
| 4.2 Alloy 600 and Alloy 182: ICG-EAC Round Robin..... | 4-11 |
| 5 SCC Crack-Growth-Rate Testing of Alloy 690 and Its Weld Metals..... | 5-1 |
| 5.1 Materials | 5-1 |
| 5.2 Alloy 152 Crack-Growth Testing | 5-3 |
| 5.3 Alloy 690 Crack-Growth Testing | 5-6 |
| 5.4 Plans for Future Testing | 5-9 |
| 6 Materials Characterization | 6-1 |
| 6.1 Alloy 182 Weld Metal..... | 6-1 |
| 6.2 Alloy 690 CRDM Tubing Heats..... | 6-3 |
| 6.3 Alloy 152 Weld Metal..... | 6-3 |
| 6.4 Crack-Tip Examinations | 6-8 |
| 7 Conclusions..... | 7-1 |

Figures

| | | |
|------|--|------|
| 2-1 | Water Flow Diagram of PNNL Crack-Growth Systems..... | 2-2 |
| 2-2 | Crack-Growth-Rate Test Frame Loading System..... | 2-3 |
| 2-3 | Schematic of dcpd System | 2-4 |
| 3-1 | Test Sample Pre-Cracking Station..... | 3-1 |
| 3-2 | Water Make-Up Board is Shown that Produces Ultra-High-Purity Water at a Resistance of 18.18 M ohm-cm | 3-2 |
| 3-3 | System #1 Water Board Shown During Initial Assembly | 3-3 |
| 3-4 | Crack-Growth Test System #1 when it was Near Completion and Before the Initial Shakedown Test..... | 3-4 |
| 3-5 | Systems #1 and #2 Shown During High-Temperature Testing..... | 3-5 |
| 3-6 | Systems #3 Housed in Radiological Lab Space Capable of Testing Samples with Low Activation Levels | 3-6 |
| 3-7 | Schematic Drawing of a 0.5T CT Specimen is Shown | 3-7 |
| 3-8 | Two CT Samples Mounted in Series Prior to SCC Crack-Growth Testing..... | 3-8 |
| 3-9 | Air Fatigue Test of CT009 for dcpd Calibration | 3-11 |
| 3-10 | Air Fatigue Test of CT010 for dcpd Calibration | 3-11 |
| 3-11 | Macrograph Showing Beach Marks on Crack Growth Surface of CT010 Sample | 3-12 |
| 3-12 | Crack Length Data during One of the Beach Mark Phases of the CT009 Air Fatigue Test..... | 3-13 |
| 3-13 | Example of Crack-Length Resolution during SCC Test on CW316SS under Constant K Conditions in Simulated BWR Water | 3-13 |
| 3-14 | Example of Crack-Length Resolution during SCC Test on Alloy 182 under Constant K Conditions in Simulated PWR Water | 3-14 |
| 3-15 | Outlet Water Conductivity as a Function of Test Time for Shakedown Test in System #1..... | 3-15 |
| 3-16 | Axial Temperature Profile in Autoclave under BWR Testing Conditions..... | 3-16 |
| 3-17 | Outlet Water Conductivity as a Function of Test Time for Shakedown Tests in Systems #2 and #3 | 3-17 |
| 3-18 | Autoclave Interior Axial Temperature Profile during a PWR Test at 325°C (617°F). | 3-18 |
| 4-1 | Pre-Cracking Response for CW316SS Sample CT001..... | 4-2 |
| 4-2 | Overall SCC Crack-Growth Response for CW316SS in Test CT001 | 4-2 |
| 4-3 | Air Pre-Cracking of Sample CT003..... | 4-4 |
| 4-4 | Air Pre-Cracking of Sample CT004..... | 4-4 |
| 4-5 | Crack-Transitioning Steps for Samples CT003 and CT004 Tested in Series | 4-5 |

| | | |
|------|--|------|
| 4-6 | Overview of SCC CGR Response under Constant K Condition Switching from BWR Oxidizing to BWR HWC for CT003 and CT004 Tested in Series | 4-5 |
| 4-7 | Crack-Growth Test for CT005 Sample | 4-6 |
| 4-8 | Crack Length, Electrochemical Potential, and Outlet Conductivity Plotted Versus Test Time for the CW316LSS Sample. | 4-8 |
| 4-9 | Crack Length, Electrochemical Potential, and Outlet Conductivity Plotted Versus Test Time for the CW316LSS Sample. | 4-8 |
| 4-10 | Optical Micrographs Showing Cracks From the Inside Surface of the CW 316LSS CT008 Test Sample. | 4-9 |
| 4-11 | Scanning Electron Micrographs Showing Mixed-Mode, IG/TG Fracture Surface Morphology for CW316LSS CT008 Sample. | 4-10 |
| 4-12 | Summary of PNNL Measured Crack-Growth-Rate Data for CW316SS Heats Showing High Propagation Rates for the One Heat under HWC Conditions. | 4-10 |
| 4-13 | In-situ Pre-Cracking and Crack Transitioning Steps for Alloy 600 Test | 4-11 |
| 4-14 | Alloy 600 CGR Test Results Following Round-Robin Prescribed Steps | 4-12 |
| 4-15 | Optical Micrograph Showing Fracture Surface for Alloy 600 Round-Round Sample tested in Simulated BWR Oxidizing Water with 30 ppb Sulfate Added | 4-13 |
| 4-16 | Pre-Cracking and Transitioning Stages for Alloy 182 Test in BWR Oxidizing Water | 4-14 |
| 4-17 | Crack-Growth Response for Alloy 182 in BWR Oxidizing Water During Steps Under Constant K and then with Cyclic Loading with a Hold Time. | 4-14 |
| 4-18 | Crack Transitioning Stages for Alloy 182 Round Robin Test in PWR-Simulated Primary Water at 325°C (617°F). | 4-15 |
| 4-19 | Hydrogen Effects on SCC CGR of Alloy 182 under Constant K Conditions..... | 4-16 |
| 5-1 | Four of the Alloy 690 CRDM Tubes Received at PNNL | 5-2 |
| 5-2 | Sectioning Diagram for the 152 Welded Block. | 5-3 |
| 5-3 | Optical Micrograph of Section C Showing the Location of the Machined Notch | 5-3 |
| 5-4 | Intended Pre-Crack Increments for CT013 Alloy 152 MHI Mock-Up Weld Crack-Growth Test Being Conducted in NRC System #1 | 5-4 |
| 5-5 | Pre-Cracking and Initial Crack Transitioning for the First Alloy 152 CGR Test in PWR-Simulated Primary Water at 325°C (617°F). | 5-5 |
| 5-6 | Crack Transitioning for the First Alloy 152 CGR Test in PWR-Simulated Primary Water at 325°C (617°F). | 5-5 |
| 5-7 | Expanded View of Final Crack Transitioning Step in the First Alloy 152 Test. The test is on-going. | 5-6 |
| 5-8 | Image Showing the Two Alloy 690, 0.5T CT Samples Mounted in Series Within SCC CGR Test System #3 | 5-7 |
| 5-9 | Air Fatigue Pre-Cracking of Alloy 690 Samples to be Tested in Series | 5-8 |
| 5-10 | Initial Crack Transitioning Step for Alloy 690 Samples Tested in Series..... | 5-9 |

| | | |
|------|---|------|
| 6-1 | SEM Backscatter Electron Images Showing Elongated Grain Structure in the Round-Robin Alloy 182 Weld Metal. | 6-1 |
| 6-2 | SEM Backscatter Electron Images Showing “Crenulated” Boundaries Caused by Presence of Carbide Precipitates. | 6-2 |
| 6-3 | TEM Brightfield Images Illustrating High Dislocation Densities in Most Regions and $M_{23}C_6$ and MC Carbides in the Matrix and at Grain Boundaries | 6-2 |
| 6-4 | TEM Darkfield Images Showing High Density of Fine $M_{23}C_6$ and MC Carbides at Grain Boundaries. | 6-3 |
| 6-5 | Optical Metallographs Showing Grain Structures for Alloy 690 Heat RE243 in the Transverse, Longitudinal, and Circumferential Orientations. | 6-4 |
| 6-6 | Optical Metallographs Showing Grain Structures for Alloy 690 Heats WP016, WP140, and RE169 | 6-4 |
| 6-7 | SEM Micrographs of the Alloy 152 Weld Showing Long Dendrites and Much Smaller, Equiaxed Dendrites..... | 6-5 |
| 6-8 | Scanning Electron Microscope Images are shown from the Alloy 152 Weld Material..... | 6-6 |
| 6-9 | SEM Secondary-Electron Image is shown Along with Composition Maps for Mn, Nb and Al..... | 6-7 |
| 6-10 | An Example of a Different Dendritic Boundary that Shows a Single Large Cr-carbide, with Numerous Smaller Nb-carbides along the Boundary..... | 6-7 |
| 6-11 | Compositional Maps Taken in STEM Mode from the JEOL 2010F Transmission Electron Microscope Revealed that Both Cr- and Nb-rich Carbides are Present on the Boundary Between Two Dendrites..... | 6-8 |
| 6-12 | Overall Composite Image of Crack in Cross-Section for Crack-Growth Sample CT005..... | 6-11 |
| 6-13 | Crack Wall Oxides in Cold-Worked 316LSS Test Sample CT005..... | 6-12 |
| 6-14 | Crack Tip#1 in Cold-Worked 316LSS Test Sample CT005..... | 6-13 |
| 6-15 | Crack Tip #2 in Cold-Worked 316LSS Test Sample CT005..... | 6-14 |

Tables

| | | |
|-----|--|------|
| 3-1 | A Typical Pre-Cracking and Crack-Transitioning Procedure Used by PNNL for Subsequent SCC Crack-Growth Testing at $30 \text{ MPa}\sqrt{\text{m}}$ ($27.2 \text{ ksi}\sqrt{\text{in}}$)..... | 3-9 |
| 3-2 | Comparison of dcpd and Actual Crack Length Measurements..... | 3-12 |
| 4-1 | Type 316SS Heats..... | 4-1 |
| 5-1 | Alloy 690 and 152 Test Materials..... | 5-1 |

Executive Summary

Stress-corrosion cracking (SCC) of nickel- and iron-base stainless alloys has been evaluated in simulated light-water-reactor environments. A critical accomplishment in the first phase of this project was the design and construction of state-of-the-art, crack-growth-rate (CGR) test systems capable of experimentation in ultra-high-purity or tailored water chemistries at temperatures up to 360°C. High-resolution, direct current potential drop (dcpd) is used to measure crack length in-situ and enable interactive control of loading conditions. Testing capabilities were demonstrated and qualified through experiments on cold-worked (CW) stainless steels, CW alloy 600, and alloy 182 weld metal as part of round-robin collaborations.

The CGR tests on stainless steels evaluated stress intensity, cyclic loading, oxygen and hydrogen concentration, electrochemical potential (ECP), and sulfate additions on SCC propagation rates. Tests documented accurate control of mechanical and environmental conditions plus reproducible dcpd crack-length measurements with resolution down to μm dimensions. Three tests on two different CW316SS heats exhibited the expected benefit when adding H_2 and removing O_2 from the water with CGRs decreasing by a factor of 50–100 times. This CGR response when changing from simulated boiling-water reactor (BWR) oxidizing to hydrogen water chemistry (HWC) conditions was repeated several times during a single experiment. The ability to test two fully instrumented and controlled samples in series was also demonstrated. Surprisingly, high CGRs at low ECPs were observed for one CW316LSS heat. Two samples of this material were tested in different systems over a range of stress intensities and hydrogen levels. Only a small decrease (2–3X) was seen at HWC in comparison to BWR oxidizing conditions (2000 ppb O_2). A final step in establishing testing capabilities was CGR testing as part of a round robin organized by the International Cooperative Group on Environment-Assisted Cracking (ICG-EAC) on alloy 600 and alloy 182 materials. Experiments were conducted in BWR oxidizing water for both alloys and in simulated pressurized water reactor (PWR) primary water for the alloy 182 weld metal. Results demonstrated state-of-the-art capabilities through comparisons with other laboratories in the U.S., Europe, and Japan.

The long-term emphasis for the project is the evaluation of SCC in nickel-base alloys and their weld metals. This includes some examination of current alloy 600, 182, and 82 materials, but with most tests planned for alloy 690, 152, and 52 materials. Initial SCC results are described for these materials. The influence of hydrogen concentration on CGR in PWR primary water is being studied using alloy 182 weld metal. Higher SCC propagation rates were measured as the hydrogen concentration was decreased from 29 to 12 cc/kg. This lower hydrogen level will move the ECP near the Ni/NiO transition line under these temperature and pH conditions. The first test on alloy 152 weld metal is showing stable, but slow CGR in PWR primary water at 325°C (617°F). This response has been measured under gentle cycling with a hold time, and the transition to constant K is not yet complete. Preliminary crack transitioning steps are also presented for alloy 690 control rod drive mechanism (CRDM) materials (as-received, thermally treated versus solution annealed) being tested in series. A wide range of characterization has

been performed on the project materials including optical metallography, scanning electron microscopy and transmission electron microscopy of microstructures and microchemistries. In addition, detailed examinations of fracture morphologies and crack tips were conducted to better understand SCC mechanisms.

Acknowledgments

The authors recognize technical support for the research performed including John Keaveney and Rob Seffens for crack-growth system construction and testing, Clyde Chamberlin for optical metallography, Alan Schemer-Kohrt and Ruby Ermi for scanning electron microscopy, Dan Edwards and John Vetrano for transmission electron microscopy, and Larry Thomas for analytical electron microscopy of stress-corrosion crack tips. Significant contributions were also obtained from support staff (pipe fitters, iron workers, electricians, and safety engineers) at Pacific Northwest National Laboratory during design and construction of the test systems. Critical interactions with Peter Andresen and technical staff at General Electric Global Research are also acknowledged. Their help was essential for initial system design, assembly of individual systems, and shakedown testing. Peter Andresen has been an excellent resource throughout the construction and demonstration phases of the project. The work is sponsored by the Office of Nuclear Regulatory Research, U.S. Nuclear Regulatory Commission under job code N6007 with Eric Reichelt as the project manager. Pacific Northwest National Laboratory is operated by Battelle Memorial Institute for the U.S. Department of Energy.

Acronyms and Abbreviations

| | |
|---------|--|
| ASTM | American Society for Testing and Materials |
| ATEM | analytical transmission electron microscopy |
| BSE | backscatter electron |
| BWR | boiling-water reactor |
| CGR | crack-growth rate |
| CRDM | control rod drive mechanism |
| CT | compact tension |
| CW | cold worked |
| dcpd | direct-current, potential drop |
| DOE | U.S. Department of Energy |
| ECP | electrochemical potential |
| EDS | energy-dispersive x-ray spectroscopy |
| EMF | electromagnetic field |
| EPRI | Electric Power Research Institute |
| GE | General Electric |
| GEG | General Electric Global Research |
| HWC | hydrogen water chemistry |
| ICG-EAC | International Cooperative Group on Environment-Assisted Cracking |
| IG | intergranular |
| IGSCC | intergranular stress corrosion cracking |
| K | stress intensity factor |
| LWR | light-water reactor |
| MHI | Mitsubishi Heavy Industries |
| MRP | Materials Reliability Program |
| NRC | U.S. Nuclear Regulatory Commission |
| NWC | normal water chemistry (BWR) |
| PEELS | parallel-detection electron-energy-loss spectrometer |
| PNNL | Pacific Northwest National Laboratory |
| PWR | pressurized water reactor |
| RR | round robin |
| RVCH | reactor vessel closure head |
| SA | solution annealed |
| SCC | stress corrosion cracking |
| SE | secondary electron |

| | |
|------|---|
| SEM | scanning electron microscopy |
| STEM | scanning transmission electron microscopy |
| TEM | transmission electron microscopy |
| TG | transgranular |

1 Introduction

Engineering research has clearly demonstrated the practical importance of crack-growth-rate (CGR) testing to quantitatively assess structural materials resistance to environment-assisted cracking and enable effective assessment/prediction of performance. In particular, recent observations of stress-corrosion cracking (SCC) in PWR vessel-head penetrations point out the need for reliable data on both nickel-base alloys and their weldments. While several laboratories worldwide have attempted to conduct effective crack-growth experimentation, few have been able to produce consistent quantitative response. This has resulted in a number of international group programs and round robins to help “standardize” processes to achieve high-quality data. The technical lead for most of these activities has been General Electric (GE) Global Research who has been at the forefront of SCC CGR testing.

Despite many data quality issues, laboratory testing has been used to establish SCC CGR characteristics of nickel-base stainless alloys in light-water-reactor (LWR) environments. A suitable reference curve for alloy 600 is described in Materials Reliability Program (MRP) document MRP-55. The MRP-55 postulates the use of a reference curve for crack growth of mill-annealed alloy 600 in PWR environments with a CGR of 4.3×10^{-8} mm/s at a stress intensity factor (K) of 20 MPa \sqrt{m} (18.2 ksi \sqrt{in}) at 325°C (617°F). Results for alloy 182 show propagation rates nearly five times higher than for the alloy 600 at comparable test conditions. The MRP has also compiled CGRs for alloy 690 that suggest growth rates on the order of 25–30 times slower than those for alloy 600. A parallel figure of merit for alloy 152 is not available, but that alloy is likely to have lower CGRs than alloy 182 and perhaps be comparable to that for alloy 690. The goal of the present project is to assist the U.S. Nuclear Regulatory Commission (NRC) in generating CGR data on alloy 690 and its weld materials to better define their SCC response. Some crack growth testing may also be performed on alloy 600 and 182 samples. Specimens will be taken from a variety of sources including control rod drive mechanism (CRDM) tubing, plate material, mockup welds and from components removed from LWR service.

Alloy 690 and its welds pose significant challenges for the quantitative measurement of SCC CGRs. First, the very low propagation rates expected for these materials make it difficult to perform a test in a reasonable amount of time. Pragmatic laboratory testing of SCC-CGR behavior requires a uniform (i.e., not segmented or excessively “fingered”) crack extension of several grain diameters (50–100 μm) in order to obtain an accurate evaluation of crack propagation. Ideally, this response should be reproduced during the test. However, if the material has a CGR of 1×10^{-9} mm/s, then it would take roughly 3 years to extend the crack by 100 μm . Even with compromise in the amount of crack length extension, tests of alloy 690 and its weld metals are likely to take at least 6 months per sample to establish a rate a constant K under a single environmental condition with 9–12 months probably needed when including pre-cracking and transitioning steps. Even for this case, excellent crack-length resolution is essential. A rate of 1×10^{-9} mm/s can only be determined accurately in a reasonable amount of time (months) if the noise in the crack-length data is in the 1 μm range. System reliability is another less-often-considered issue. A continuous test for 6–12 months requires reliable equipment, online monitoring of performance, and designs for efficient replacement of parts

without stopping the test. Because some materials may have CGRs that are below 1×10^{-9} mm/s under constant K conditions, a standardized set of testing conditions must be determined that will allow a consistent basis of comparison for different materials and environmental conditions. This will include different cyclic loading conditions and hold times facilitating the effective transition from fatigue to corrosion fatigue to SCC propagation. Thus, successful evaluation of these very low CGR materials truly requires state-of-the-art equipment and techniques that provide for a means to obtain quantitative assessment of environment-assisted cracking response.

In order to address the key issues above, three SCC CGR systems have been designed and assembled at Pacific Northwest National Laboratory (PNNL) specifically for testing in high-temperature, simulated BWR or PWR primary-water coolants. Each CGR test system is able to test a single 1T compact tension (CT) sample or at least two 0.5T CT samples simultaneously at test temperatures up to 360°C (680°F). The autoclaves and the water make-up systems have the capability to effectively simulate high-purity BWR or PWR water as well as control levels of oxygen, hydrogen, and selected impurities. Control of hydrogen over pressure in PWR primary water will be sufficient to alter the nickel-base alloy electrochemical potential (ECP) from well above to below the Ni/NiO transition for near-neutral pH. The systems use reversing direct-current, potential drop (dcpd) for crack-length measurement and active load/K-control along with in-situ measurement capability for temperature and ECP. One CGR system was assembled in a radiological space and is capable of testing metallic alloys with low activity levels (e.g., samples machined from components removed from LWR service). Round-robin tests have been conducted on austenitic stainless steels, alloy 600 and alloy 182 samples to demonstrate capabilities and establish data quality. In addition, the first experiments on alloy 690 and 152 materials have been initiated. Design and construction of the systems, CGR testing results, and materials characterization activities are described in the following sections of this Volume 1 report. Additional reports will be produced as significant accomplishments are made as part of this ongoing research at PNNL.

2 Design of SCC Crack-Growth Test Systems

The purposes of the crack-growth systems are to develop, control, and measure stress corrosion cracks under well-defined material and environmental conditions, and ensure that the SCC growth rate response is reproducible and characteristic of the test conditions. Features expected in a good crack-growth system include active constant K load control, active temperature control, a sensitive crack length measurement apparatus, a flowing high-temperature water system, control over all aspects of water chemistry, and continuous monitoring of all pertinent test parameters. The options for PNNL in creating a crack growth capability were to design our own systems, buy commercial systems, or copy a system at another research institute. It was determined very early in the program that the most advanced and reliable crack-growth systems in the world have been designed, developed, and run by Peter Andresen at General Electric Global Research (GEG). His crack-growth systems have been copied to various degrees by research institutes and commercial companies throughout the world. The decision was made to work closely with Peter Andresen and GEG staff on our system design. In the process of building the systems at PNNL, some design aspects were improved, and more up-to-date parts were chosen when advantageous. GEG has incorporated some of these improvements and newer parts into their own systems.

The key components of these systems are: (1) a servo-electric load control system capable of holding constant load for very long periods of time, (2) a high-pressure piston pump to pressurize and flow water through the high-temperature loop, (3) an autoclave, (4) a custom-made water board for water chemistry control, (5) a reversing dcpd system for crack length estimation, and (6) a continuous data acquisition system. Careful consideration has gone into the selection of each piece of equipment to optimize either test system control or test environment. Some of the most important optimizations were to: (1) make sure that all wetted components release no contamination into the water, (2) have a high water flow rate through the autoclave, (3) have uniform temperature through a large volume of the autoclave, (4) have consistent water pressure, (5) have highly accurate measurements of test environment (temperature, conductivity, pH, load, dissolved gas content), and (6) have a sensitive dcpc measurement system. Each of the subsystems will be discussed in further detail below.

The water flow design of the system is a loop within a loop as shown in Figure 2.1. One loop is at low pressure, and its purpose is to flow water through a water column where selected gases and ionic impurities are dissolved or injected into the water. A side stream is taken off this low-pressure loop and fed into a high-pressure piston pump. The large pressure pulses and flow surges created by the piston pump are dampened by the use of pulsation dampers both at the inlet and outlet of the pump. The high-pressure water flows into a regenerative heat exchanger where hot water leaving the autoclave is used to heat the incoming water. Just prior to the water entering the autoclave, the partially heated water is brought up to test temperature using a preheater. After the water flows through the heated autoclave, it goes back through the regenerative heat exchanger and then through a water cooler that brings the water back down to room temperature. The cooled water then passes through a back-pressure regulator and emerges at around 10 psi of pressure. The water flows through a flow meter, a conductivity

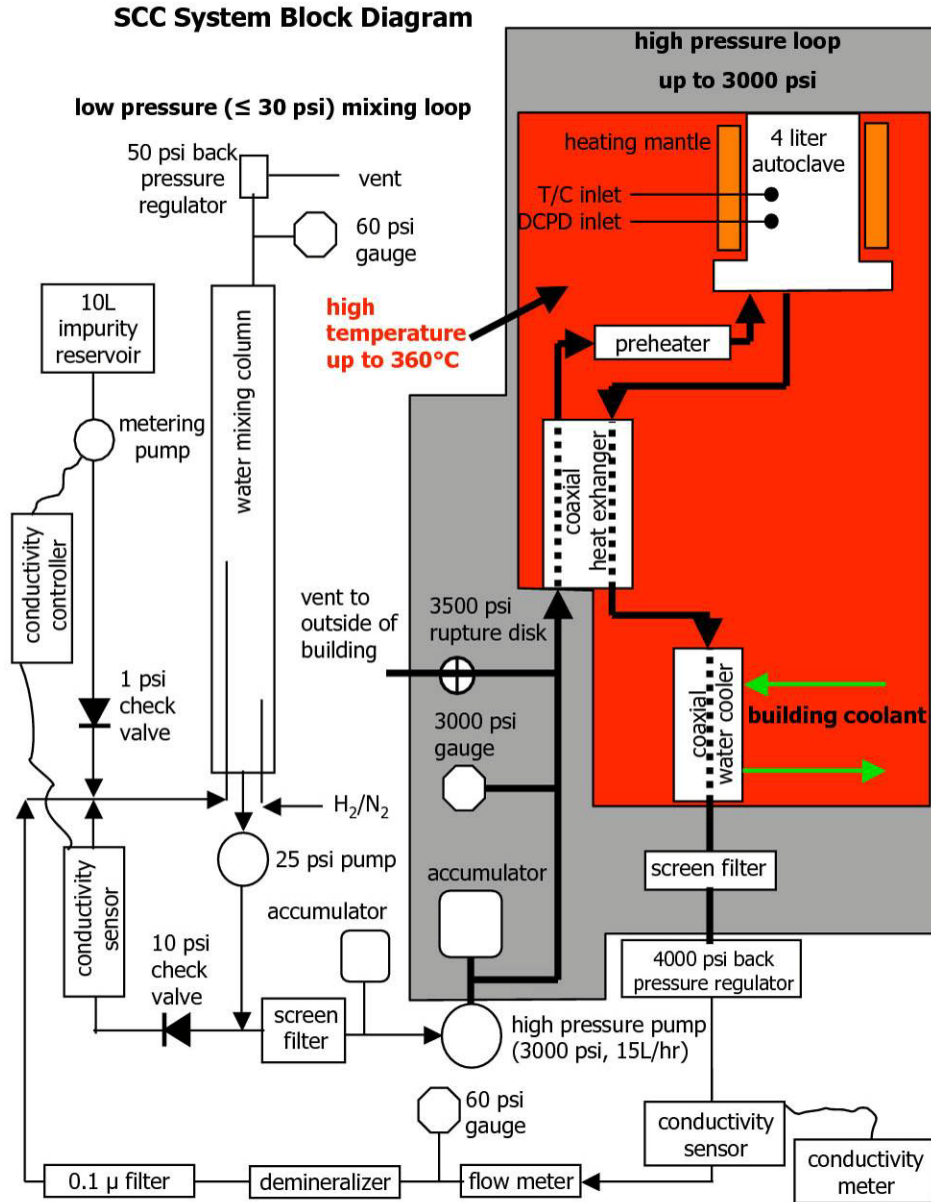


Figure 2-1 Water Flow Diagram of PNNL Crack-Growth Systems

sensor, a mixed resin bed demineralizer, and is finally dumped back into the low-pressure chemistry mixing control loop.

Boron and Li levels for PWR water testing are controlled by pre-saturating the mixed resin bed demineralizer with boric acid and lithium hydroxide to specific levels that will result in tailored near-constant B and Li content in the water. There is some drift in the Li level in the water because it is singly ionized and is easily displaced from the demineralizer by more highly positively ionized species coming off the autoclave such as chromate. The displaced Li is removed by periodic partial replacement of water in the mixing loop with water having little or no Li (and some B). Boron and Li levels in the mixing loop are determined using pHSC4 software

(obtained from Rick Eaker of Duke Power) that determines B and Li content from simultaneous measurement of water conductivity, pH, and temperature.

Load is applied to a sample using a servo-electric motor attached to the test frame. The servo-electric motor is controlled using proprietary software from GEG. The servo-electric motor has the capability to cycle the load up to about 2 Hz, allowing in-situ pre-cracking of a test sample. Using dcpd data, the GEG software can continuously adjust the servo-electric motor to provide constant K loading conditions. As shown in Figure 2.2, the load from the servo-electric motor is transmitted into the autoclave with a pullrod, and the sample is braced from above by a top plate and 4-bar linkage that transmits load to the baseplate of the autoclave which is bolted to the test frame.

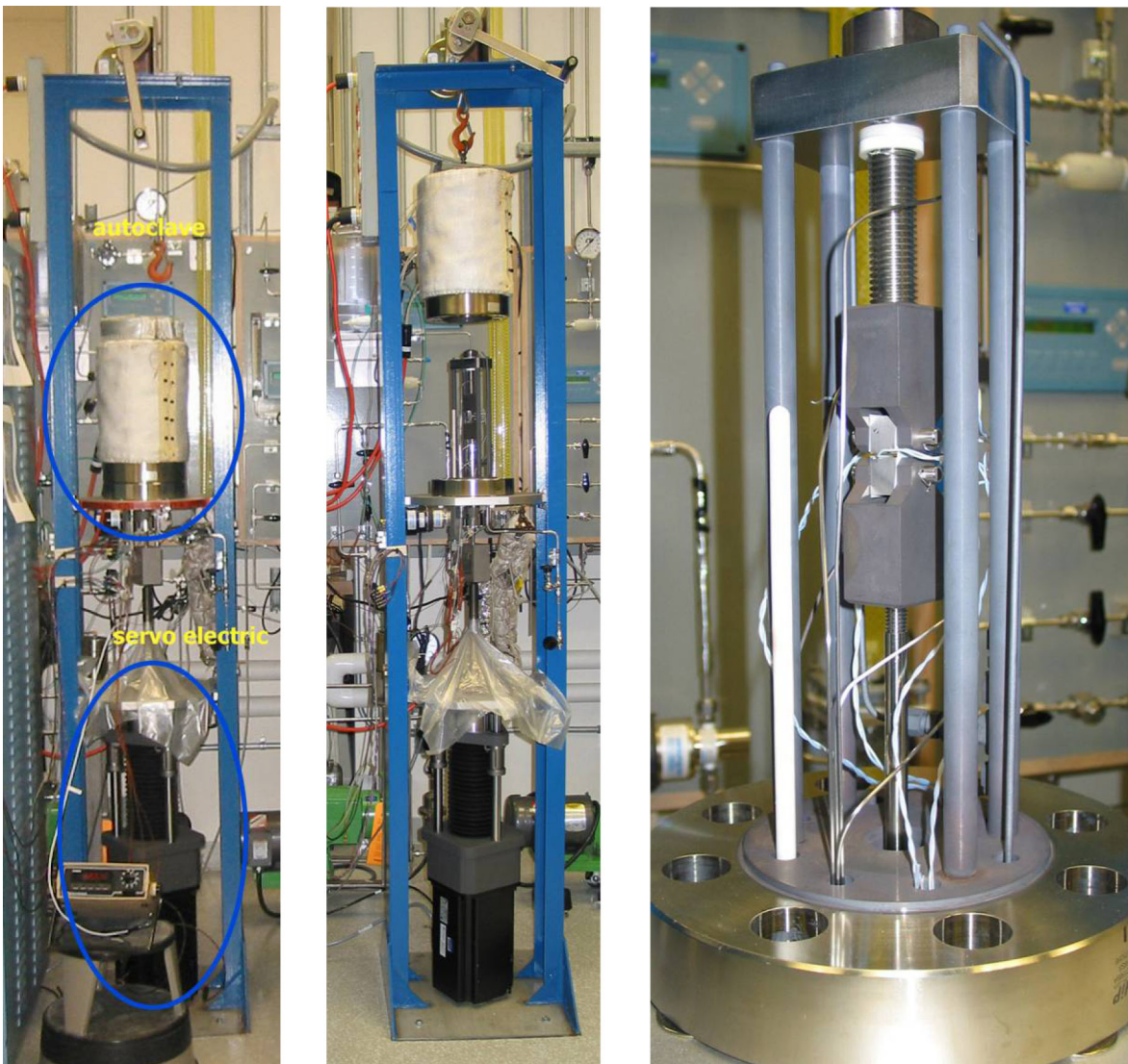


Figure 2-2 Crack-Growth-Rate Test Frame Loading System

Crack length is estimated using a reversing dcpd system developed by Peter Andresen of GEG that has an advertised sensitivity of $\sim 1 \mu\text{m}$ change in crack length. A sketch of the system is shown in Figure 2.3. As with all DC potential drop measurement systems, a constant current is run through the sample, and the voltage across the crack plane is measured and converted into a crack length by means of an empirically derived formula relating voltage to crack length. Using a solid-state polarity-reversing switch built into the current path, potential drop is measured in both a forward and reverse current flow condition. By measuring in both directions, the system eliminates contact voltages from the measurement.

The GEG software also controls the operation of the dcpd system. A wide range of measurement intervals can be selected. The most common is to set the system to measure voltage twice per second. Platinum wire is used for current and voltage feeds into the autoclave. The Pt wire feeds for BWR testing are insulated in pure Teflon shrink wrap, and to help reduce sensitivity to external electromagnetic fields (EMFs), the Teflon-coated wire pairs are twisted together both inside and outside the autoclave. For PWR testing where the water temperature exceeds the operational limit of polytetrafluoroethylene (PTFE [Teflon]), segmented

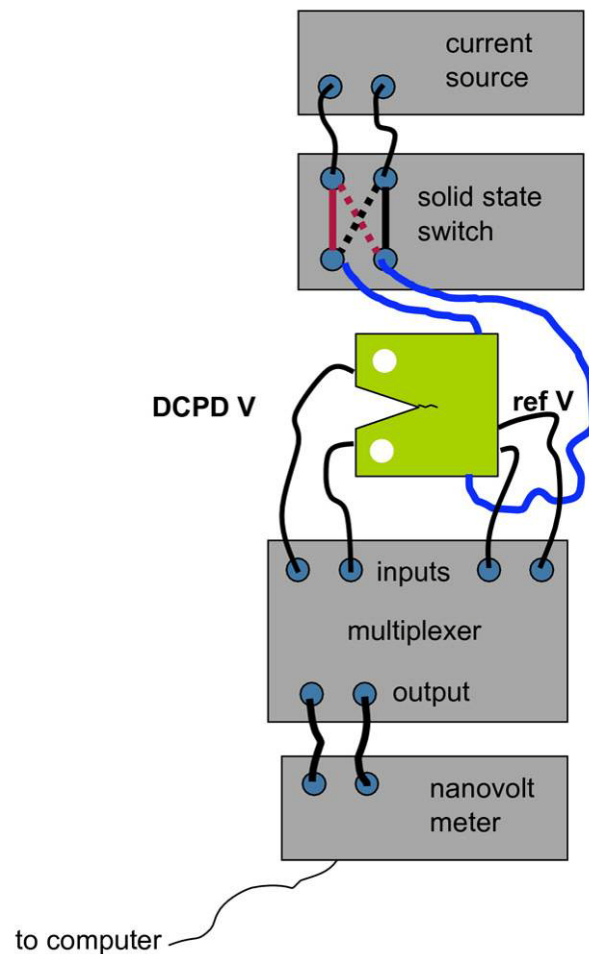


Figure 2-3 Schematic of dcpd System

ceramic tubing is used to insulate the wire inside the autoclave. The segmented insulation allows some crosstalk in the voltage wires that is minimized by keeping the wires separated as far as reasonably possible. In addition, the current wires are kept away from the voltage measurement wires. The sample is electrically insulated from the load train through a combination of ceramic and Teflon spacers and sleeves. Spot welding is used to attach the platinum wires to a specimen. The spot weld locations are marked on the sample prior to inserting the sample into the load train.

The PNNL systems have the capability to monitor autoclave water outlet conductivity, mixing loop water conductivity, autoclave temperature, autoclave water flow rate, sample corrosion potential (via a ZrO_2 insulated Cu/Cu_2O reference electrode in the autoclave), dissolved oxygen, water pressure, dcpd current, and dcpd voltage. With the exception of water pressure and flow rate, these parameters are recorded in the test data file. Statistical information on temperature and current fluctuations are also recorded. Additionally, messages describing changes in test conditions and other issues are a permanent part of the data record.

3 Construction and Shakedown Testing of SCC Crack-Growth Systems

3.1 Construction and Assembly Activities

Construction of the three test systems took place over an 18-month period with the first system being completed in March 2005, the second system completed in October 2005, and the third system completed in June 2006. While a general template and a parts list was obtained from GEG, neither piece of information was complete. Large amounts of time went into determining the necessary features for many of the parts. In some cases, parts on the list were found to be out-of-date, and replacement parts had to be found. While the PNNL test systems have the same components and conceptual design as the GEG systems, a standard system layout did not exist, and we designed our own to best fit within the available lab space. Clean tools and rubber gloves were used during the water board construction so that the test systems would have the highest possible water purity. A GEG technician, and later, Peter Andresen, visited PNNL to help with certain key undocumented construction methods during the final fabrication phases of the first test system.

A series of pictures showing individual parts of the PNNL test systems and supporting facilities are shown in Figures 3.1 through 3.6. These images give an overview of the various pieces of equipment, and captions describe each component.



Figure 3-1 Test Sample Pre-Cracking Station. This Instron load frame can be used to pre-crack a specimen prior to inserting the specimen into a CGR test system. Leads for dcpd attach to a sample and to the electronics in the upper-left corner of the picture.

Numerous activities and modifications were required to optimize performance for System #1. The biggest challenge with the first system was found to be maintaining an adequate water flow rate through the autoclave. After many adjustments to the high-pressure pump and the addition of a pulsation damper at the inlet of the pump, a consistent flow rate was achieved. Many other more mundane activities (such as chasing down leaks and learning how to adapt new equipment to the crack-growth system) took place. These individual activities had only minor impact on system performance, but overall represented the accumulation of key experience that was used during assembly and optimization of the second and third systems. New features that have gone into the newer systems are being retrofitted to the older systems as time permits.



Figure 3-2 Water Make-Up Board is Shown that Produces Ultra-High-Purity Water at a Resistance of 18.18 M ohm-cm. Major components include a UV light box to kill organics, a demineralizer to catch ionic solutes, a submicron filter to catch small inert particles, and a conductivity sensor to measure resistance of the water.



Figure 3-3 System #1 Water Board Shown During Initial Assembly



Figure 3-4 Crack-Growth Test System #1 when it was Near Completion and Before the Initial Shakedown Test. Green item on floor is the high-pressure (3000 psi) pump. Off-white jacket is the heating blanket that surrounds the autoclave lid (not shown). Blue frame is the load frame.



Figure 3-5 Systems #1 and #2 Shown During High-Temperature Testing



Figure 3-6 Systems #3 Housed in Radiological Lab Space Capable of Testing Samples with Low Activation Levels

3.2 General SCC Crack-Growth Testing Approach

Although systems have been designed for both 1T and 0.5T CT specimens, the primary specimen geometry to be used in this project is the 0.5T CT with side grooves. The details of the specimen geometry are shown in Figure 3.7. Prior to loading a specimen in the autoclave, the sample thickness, notch depth, a_0 , and W values are all measured and recorded into the data record for the test. Using the sample dimensions and the strength of the specimen at the test temperature, in accordance with American Society for Testing and Materials (ASTM) E-1681, an upper limit on K_{EAC} value is calculated using the formula:



Figure 3-8 Two CT Samples Mounted in Series Prior to SCC Crack-Growth Testing. The bright, non-oxidized autoclave load train indicates first usage of this test system.

Typically, this means producing initial pre-cracks of ~1 mm in length in air followed by an additional ~1 mm by cycling in-situ before transitioning to cyclic load plus hold times to promote SCC.

Practically speaking, CT samples slated for testing in series could be individually pre-cracked in-situ. However, this would result in a significant increase in system set-up requirements, sample modifications, test time and expense. The initial pre-cracking in air is now done without impacting the current operation of our 3 test systems. This pre-cracking is done under well-controlled conditions, and we make sure that samples, grips and other components are cleaned before testing.

As shown in Figure 3.1, an Instron servohydraulic test frame is used to pre-crack CT specimens in air. The same dcpd electronics and system control software in the crack-growth systems are used to control the Instron test frame making the in-situ and ex-situ pre-cracking procedure the same. The first step in pre-cracking is to cycle the sample at a relatively high frequency (1–2 Hz) with a large load ratio and K_{max} less than the K level chosen for constant K. As the crack begins to grow from the notch, the load ratio and frequency are reduced while the K_{max} value is increased. By pre-cracking in this way, each pre-crack segment can grow beyond the plastic zone created by the previous segment. For all samples, cyclic loading steps at frequencies of 0.1 Hz down to 0.001 Hz are performed in high-temperature water. The final phase involves crack transitioning by very slow cycling with a hold time ranging from 9000 s (2.5 h) to 86,400 s (24 h). This grows the crack beyond the pre-cracking plastic zone and allows the crack to transition from transgranular (TG) fatigue to the SCC crack growth mechanism that occurs for that material under constant K conditions. An example of the typical pre-cracking and crack-transitioning steps are shown in Table 3.1.

Table 3-1 A Typical Pre-Cracking and Crack-Transitioning Procedure Used by PNNL for Subsequent SCC Crack-Growth Testing at 30 MPa \sqrt{m} (27.2 ksi \sqrt{in})

| Step # | K_{max} (MPa \sqrt{m}) | Freq (Hz) | Load Ratio (R) | Wave Type | Hold Time (s) | Crack Length Increment (mm) |
|--------|--------------------------------|--------------|-------------------|------------|------------------|--------------------------------|
| 1 | 25 | 1.5 | 0.3 | haversine | NA | 0.5 |
| 2 | 27.5 | 1.5 | 0.5 | haversine | NA | 0.3 |
| 3 | 30 | 1.5 | 0.6 | haversine | NA | 0.2 |
| 4 | 30 | 1.5 | 0.7 | haversine | NA | 0.2 |
| 5 | 30 | 0.1 | 0.7 | haversine | NA | 0.2 |
| 6 | 30 | 0.01 | 0.7 | haversine | NA | 0.2 |
| 7 | 30 | 0.001 | 0.7 | haversine | NA | 0.1 |
| 8 | 30 | 0.001 | 0.7 | trapezoid | 9000 | 0.1 |
| 9 | 30 | NA | NA | constant K | NA | NA |

For materials such as cold-worked (CW) 316SS that crack very readily, obtaining a steady crack growth rate after transitioning to constant K can easily be accomplished by following the procedure shown in Table 3.1. In the case of highly SCC-resistant materials such as alloy 690 and its welds, reaching constant K and achieving a stable, consistent propagation rate may be difficult. For these materials, a standard transitioning plan will be developed that includes steps with longer hold times prior to reaching constant K. And if consistent crack growth is not observed when reaching constant K, then some or part of the final transitioning steps may be reapplied. In the case of alloy 690 and its welds, there may be certain combinations of material and environmental conditions where no steady crack growth is observed in repeated attempts at constant K. In anticipation of this SCC behavior, propagation rates will be determined under selected cyclic loading and hold time conditions as well as constant K. The most likely values for these secondary comparison conditions will be a 0.001 Hz cycle with a hold times between 9000 s (2.5 h) and 86,400 s (24 h).

The general philosophy for testing alloy 690 and its weld metals will be to obtain baseline SCC behavior for plant materials in simulated PWR primary water and also in reasonable off-normal

material and environmental conditions. Material conditions that will be examined include solution annealing and other thermal treatments, forging, and cold rolling to alter alloy microstructure and mechanical properties. Environmental conditions will include higher test temperatures (up to 360°C), variable hydrogen content and B/Li ratios, and perhaps adding minor impurities such as sulfate. With only three test systems, it will be impossible to study all the effects over a wide range of heats/materials.

The ideal increment of crack length over which to measure a steady crack growth rate would be several grain diameters. The minimum necessary crack increment can be considered from the perspective of crack increment resolution. Crack growth rates can be treated as statistically significant when the crack growth increment is at least 10 times the limiting resolution of the technique, which for these systems is ~1 µm. In this regard, the minimum crack length increment for measuring a crack growth rate could be considered to be ~10 µm, which is less than the typical grain diameter of an alloy 690 CRDM material. With expected CGRs reaching 1×10^{-9} mm/s (or lower), waiting for 10 µm of crack growth would take more than 3.5 months. While 10 µm is an exceedingly small number, waiting four months in a single crack growth condition may be impractical with only three test systems. When the time for the pre-cracking and transitioning steps are included, the total test time could rise to well over one year. Therefore, the crack length increment over which a propagation rate will be measured will depend on testing conditions and the sample response characteristics.

3.3 Proof Testing for the DCPD System

While GEG has been refining their dcpd system for many years and has great confidence in its accuracy and resolution, it was necessary to perform verification testing of the dcpd system at PNNL. To eliminate possible environmental and specimen response effects, the dcpd system was proof tested by performing fatigue crack-growth tests on specimens in air. Two 0.5T CT samples made from cold-worked 304LSS were tested. A high load ratio was used to rapidly grow the specimen and prevent the formation of uncracked linkages in the wake of the crack. The load ratio was reduced at selected intervals to create beachmarks on the crack surface that were used to compare the dcpd result with the actual crack length. The crack growth curves for these two tests are shown in Figures 3.9 and 3.10.

The attempt at creating beachmarks in the first sample was not successful, and it was only possible to accurately determine the final crack length. Beachmarks were successfully produced on the second sample as shown in Figure 3.11. The dcpd crack length versus the actual crack length values are shown in Table 3.2 for tests CT009 and CT010. In two of the four measurements, dcpd slightly underestimated the crack length while in the final CT010 measurement, dcpd slightly overestimated the crack length. No matter what the actual crack length was, the difference between the actual crack length and the dcpd crack length was never more than 0.3 mm. The greatest error for these air fatigue tests was only 2 percent. The crack length of all the samples tested to date has also been measured and compared to the dcpd crack length in Table 3.2. In selected SCC crack-growth tests, dcpd is seen to underpredict crack length by as much as 16 percent. This clearly impacted the K value during the tests and required corrections to the data after the test was completed. The results of these individual tests will be discussed in Section 4.

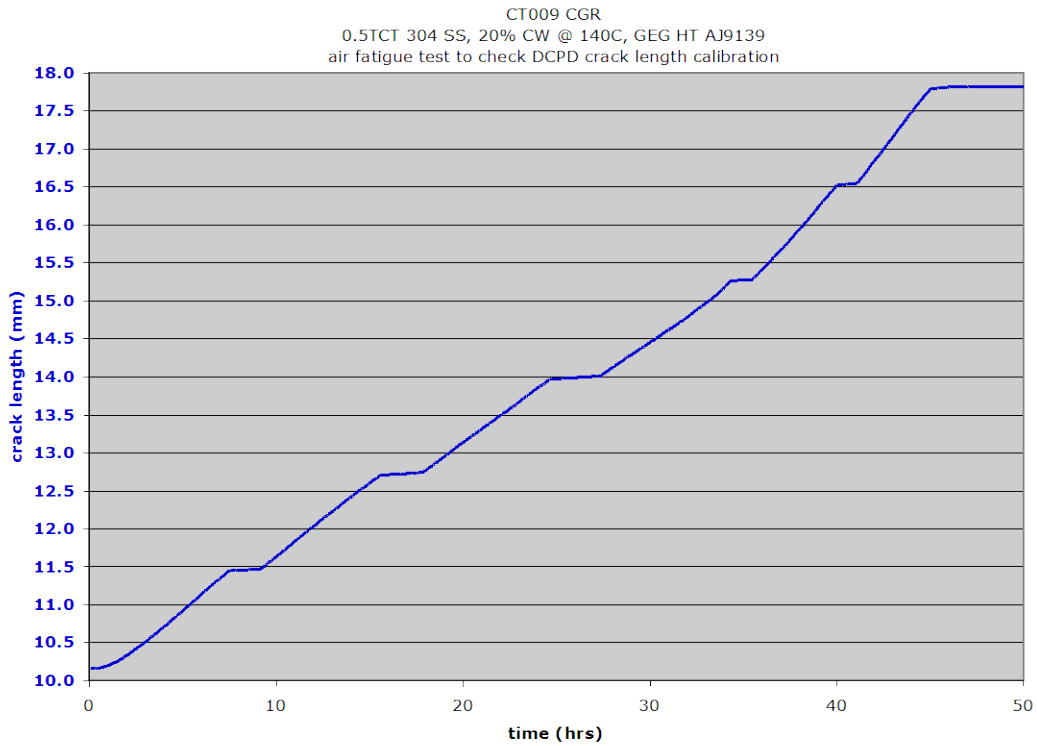


Figure 3-9 Air Fatigue Test of CT009 for dcpd Calibration

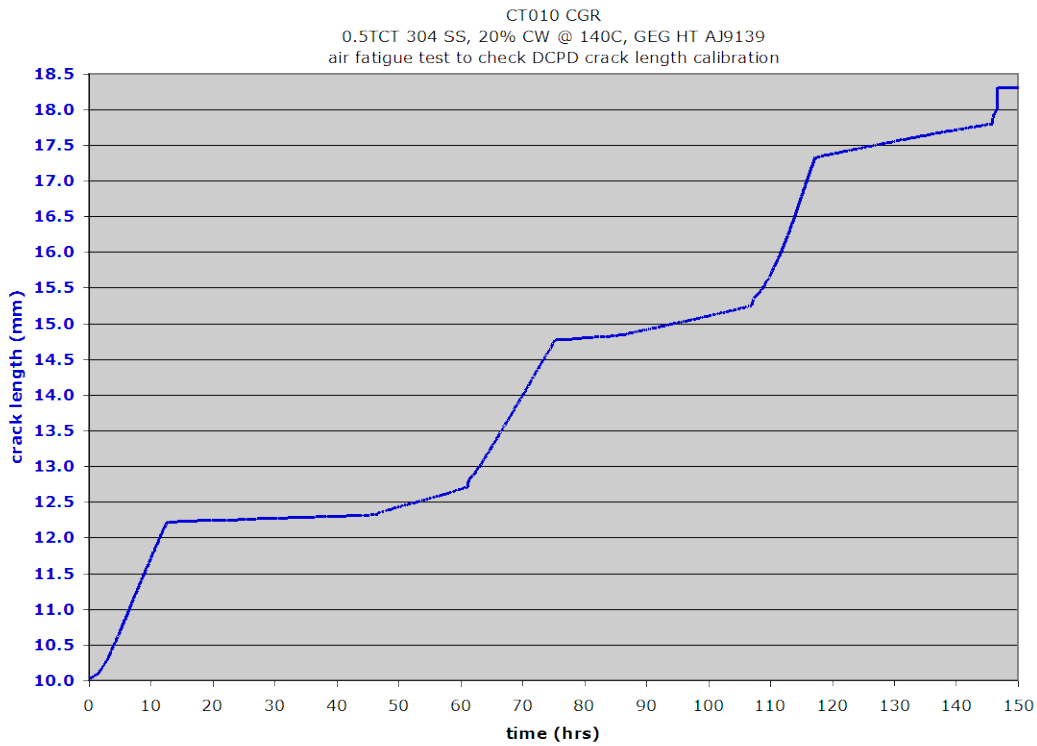


Figure 3-10 Air Fatigue Test of CT010 for dcpd Calibration

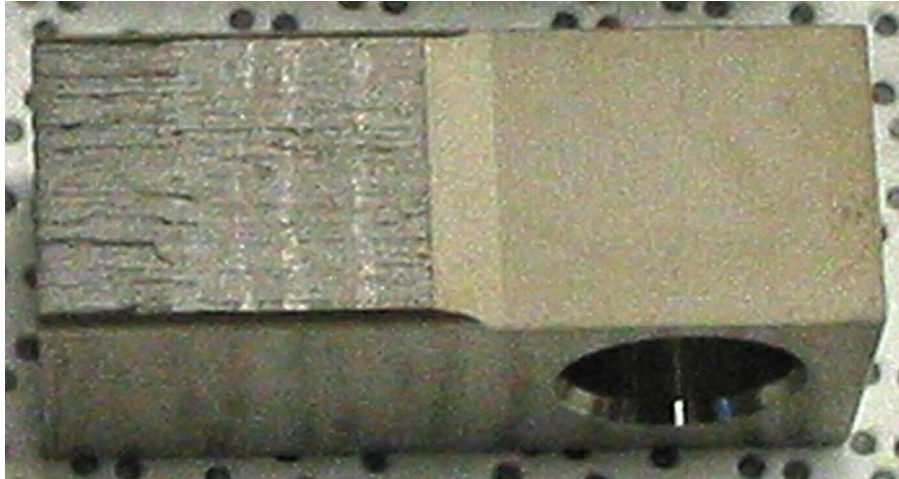


Figure 3-11 Macrograph Showing Beach Marks on Crack Growth Surface of CT010 Sample

Table 3-2 Comparison of dcpd and Actual Crack Length Measurements

| Test ID/Position | Material/Heat | Actual Crack Length (mm) | dcpd Crack Length (mm) | Difference (mm) | % Error in dcpd |
|------------------|-------------------|--------------------------|------------------------|-----------------|-----------------|
| CT001/final | CW316SS/PNNL1 | 24.1 | 24.6 | 0.4 | 2% |
| CT002/final | Alloy 600/3110439 | 17.1 | 15.4 | -1.7 | -10% |
| CT003/precrack | CW316SS/PNNL2 | 12.0 | 11.8 | -0.2 | -2% |
| CT003/final | CW316SS/PNNL2 | 16.3 | 15.2 | -1.1 | -7% |
| CT005/precrack | CW316LSS/A14128 | 12.3 | 11.9 | -0.4 | -4% |
| CT005/final | CW316LSS/A14128 | 17.2 | 14.4 | -2.8 | -16% |
| CT008/precrack | CW316LSS/A14128 | 12.3 | 12.1 | -0.2 | -2% |
| CT008/final | CW316LSS/A14128 | 16.3 | 14.3 | -2.0 | -12% |
| CT009/final | CW304SS/AJ9139 | 18.1 | 17.9 | -0.2 | -1% |
| CT010/#1 | CW304SS/AJ9139 | 12.2 | 12.2 | 0.0 | 0% |
| CT010/#2 | CW304SS/AJ9139 | 14.9 | 14.7 | -0.2 | -1% |
| CT010/#3 | CW304SS/AJ9139 | 17.0 | 17.3 | 0.3 | 2% |

Another important aspect of the dcpd system that needed evaluation was the resolution in the estimated crack length increment. The air fatigue tests serve to show the resolution attainable ex-situ. Figure 3.12 shows the crack length data during one of the beachmark phases of the CT009 air fatigue test. Under air fatigue conditions, the resolution in the estimated crack length was better than 1 μm showing that the PNNL dcpd system is sensitive to very small increases in crack length. Crack length measurement during constant K testing in BWR oxidizing conditions has slightly more scatter than during air fatigue testing giving a resolution closer to 1–2 μm as shown in Figure 3.13. A mid- 10^{-8} mm/s crack growth rate is easily resolved. Crack length resolution is similar during SCC testing of alloy 182 weld metal in PWR primary water as shown in Figure 3.14. Here the resolution is about 1 μm , and a low 10^{-9} mm/s crack growth rate is clearly resolvable (given a sufficient amount of time).

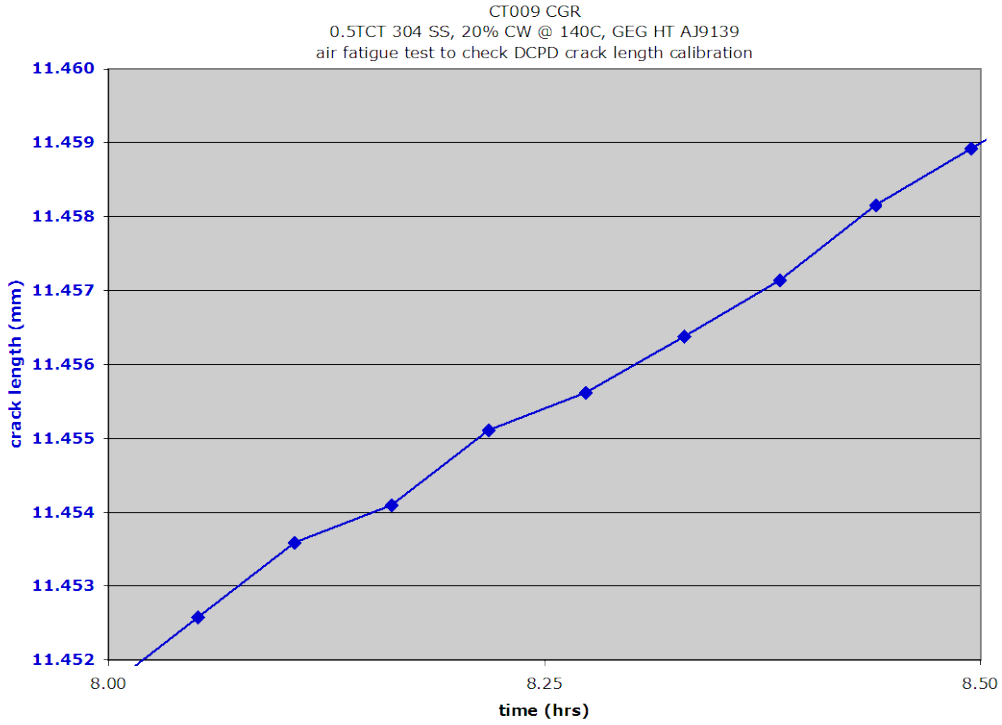


Figure 3-12 Crack Length Data during One of the Beach Mark Phases of the CT009 Air Fatigue Test. The increase in crack length shown is 7 μ m.

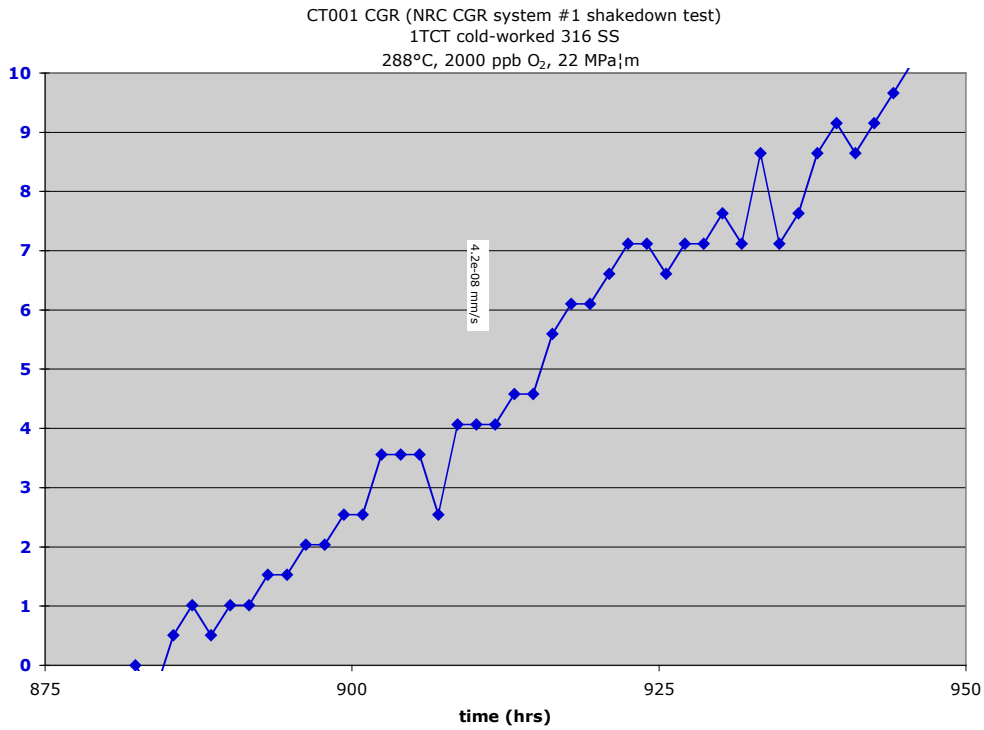


Figure 3-13 Example of Crack-Length Resolution during SCC Test on CW316SS under Constant K Conditions in Simulated BWR Water

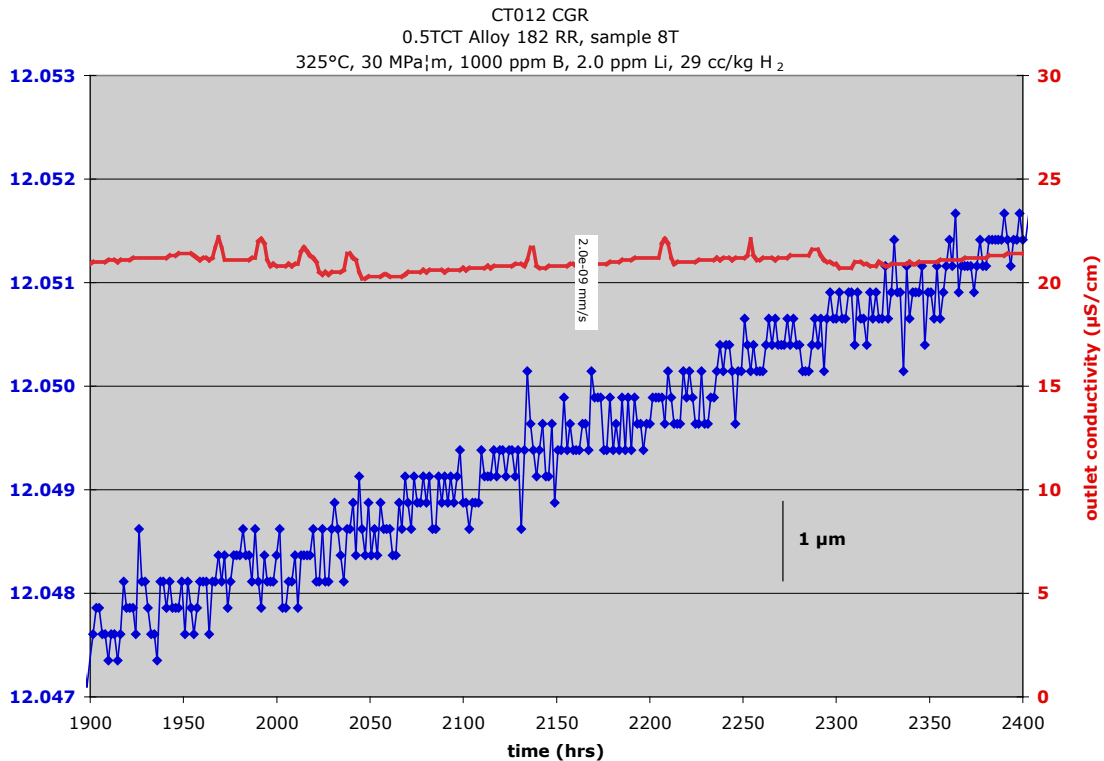


Figure 3-14 Example of Crack-Length Resolution during SCC Test on Alloy 182 under Constant K Conditions in Simulated PWR Water

3.4 Crack Growth System Shakedown Testing

After construction of each test system was completed, a shakedown test was performed using CW316SS samples. Several different heats of 316SS were used. The testing was performed with simulated BWR oxidizing conditions where the operating temperature and pressure are lower, and the water is pure. High-purity water enables the evaluation of system cleanliness, and the oxidizing conditions causes the autoclave and heated tubing to quickly form a stable oxide layer. This rapidly drops the outlet conductivity down to very low levels and establishes confidence that the system internals are not leaching impurities into the test environment. The primary goals of the shakedown tests were to clean up the autoclave water system and to verify the function of all components. Cold-worked 316SS was selected for the shakedown testing because of its well-known and consistent crack growth rate under BWR oxidizing conditions. The details of the crack growth response will be shown and discussed in detail later.

The shakedown testing of the first CGR system was a significant learning experience. The first phase was simply to ensure that the system was leak-tight at room temperature and it was run for several days at room temperature to observe the water quality and pump flow characteristics. The mixing loop water quality quickly reached 0.0555 $\mu\text{S}/\text{cm}$ that is near the value for theoretical purity water (0.0550 $\mu\text{S}/\text{cm}$). With room temperature water, the autoclave outlet conductivity reached a value of ~ 0.25 $\mu\text{S}/\text{cm}$, which was not unexpected because the water is traveling through over 10 m of non-oxidized stainless steel before reaching the outlet

conductivity sensor. When the water temperature was brought up to 288°C (550°F), the outlet water quality worsened to ~1 μS/cm and stayed there for several days. Based on prior experience at GE, we anticipated that it would take approximately 2–4 weeks for the water quality to improve to 0.1 μS/cm. However for this test system, it took over 3 months as shown in Figure 3.15. The longer-than-anticipated period of time was thought to be caused by the pulsation damper being contaminated with some grease that was being released into the water and decomposing in the autoclave. The contamination did not appear to be permanent as the outlet water quality of this test system continued to improve with subsequent crack growth tests to the point where it has stabilized at an extremely good value of 0.065 μS/cm in BWR oxidizing water.

Spatial uniformity of the water temperature under BWR conditions was also evaluated during this first shakedown test and during a subsequent BWR crack-growth test on an alloy 600 sample. An array of four bendable thermocouples was inserted into the autoclave and adjusted to measure water temperature at a total of eight locations (through two tests) along the length of the autoclave. Excellent temperature uniformity over a large distance was found as shown in Figure 3.16. The temperature measurements also show that at the base of the autoclave where the pullrod seal is located and Teflon pipe tape is used to seal the NPT feedthroughs, the temperature is well below the 300°C (572°F) maximum working temperature of PTFE.

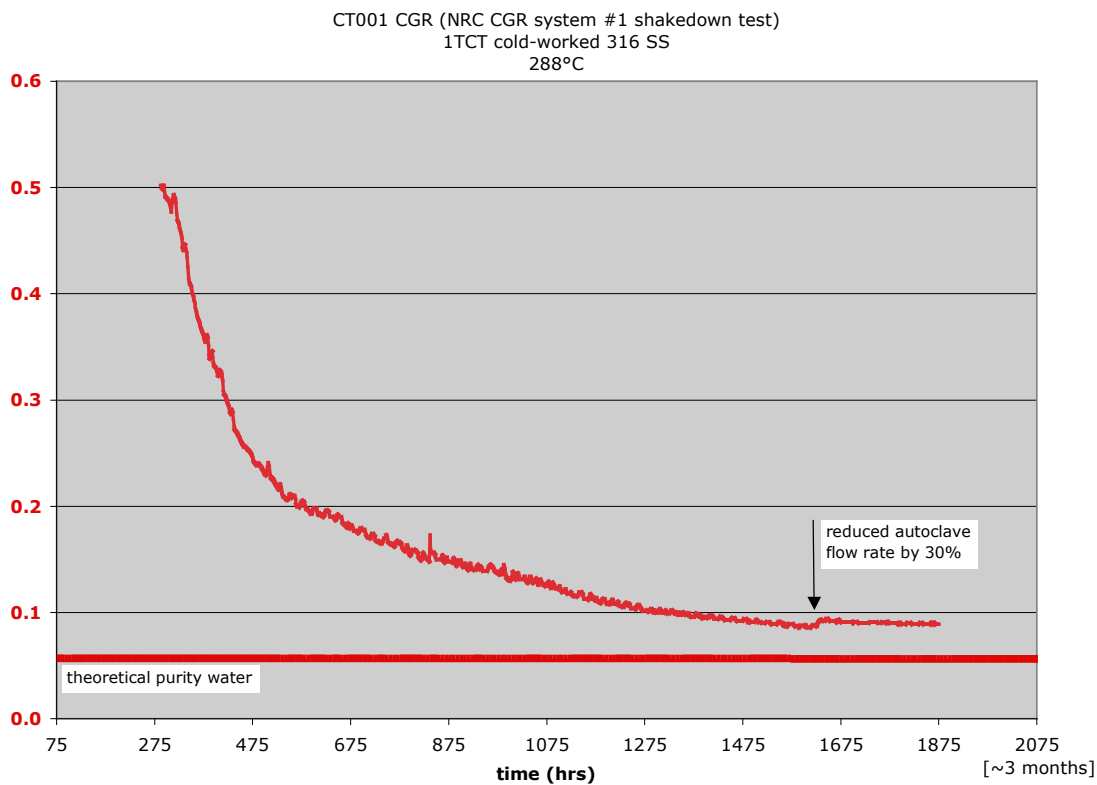


Figure 3-15 Outlet Water Conductivity as a Function of Test Time for Shakedown Test in System #1

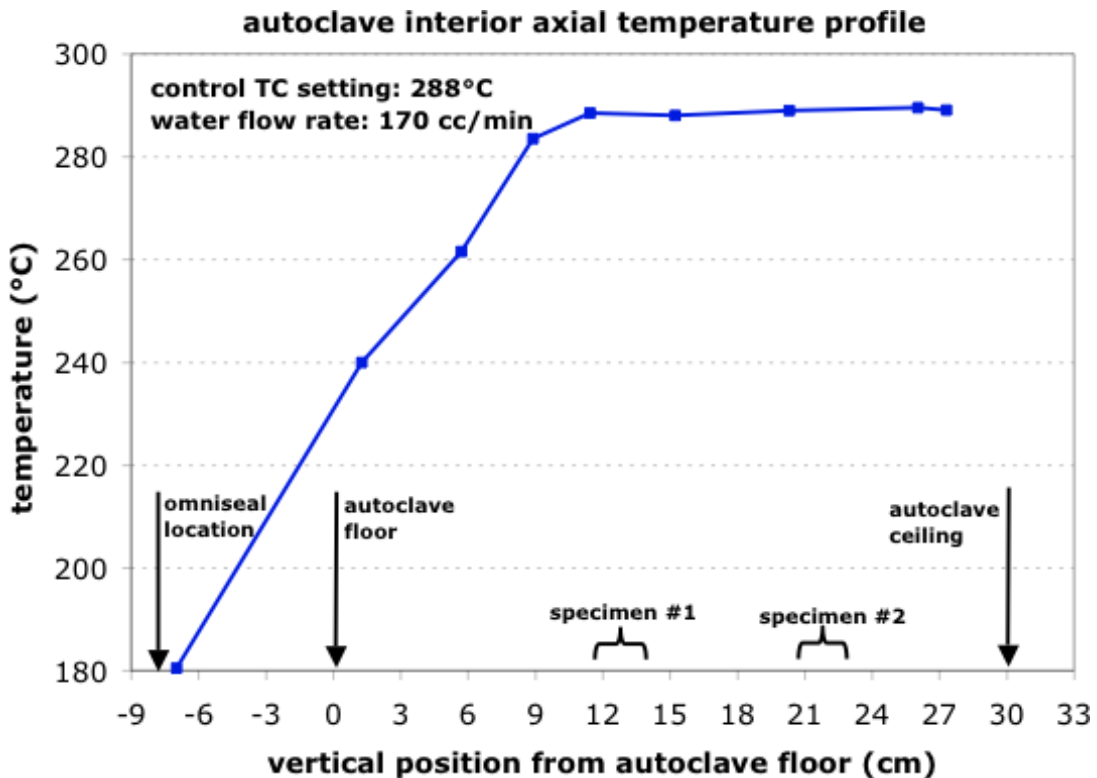


Figure 3-16 Axial Temperature Profile in Autoclave under BWR Testing Conditions

A second issue with the first test system was achieving stable high water flow through the autoclave. Despite frequent adjustment of the high-pressure pumps, it was not uncommon for the flow rate to drop off over time according to GEG staff. This was attributed, in part, to starvation of the pump during the suction stroke. GEG had attempted to mitigate the issue by installing larger diameter tubing leading to the high-pressure pump inlet and also by applying a positive water pressure at the inlet using a low-pressure continuous flow gear pump. Inspection of the inlet pressure variation of the first system at PNNL revealed, however, that despite the positive pressure and larger diameter tubing, the water pressure at the inlet of the high-pressure pump was still undergoing very large swings in pressure (varying from approximately 0 to 30 psi), which was likely causing cavitation of the water as it was being drawn into the high-pressure pump. After bringing the pressure swings under control through installation of a pulsation damper on the inlet tubing, the autoclave flow rate became much more consistent over time, and it also became possible to go to much higher flow rates with no indications of cavitation of the water at the pump inlet. The high-pressure pumps are now routinely operated at flow rates of 200–220 cc/min, and the pumps will hold this value for months at a time with very little adjustment.

Shakedown testing of the second and third systems went more quickly, even though some design modifications incorporated into these systems required observation and tuning. For the second system, the water quality went from 0.5 $\mu\text{S}/\text{cm}$ to better than 0.1 $\mu\text{S}/\text{cm}$ in only three weeks. The third system went even more quickly with the water conductivity dropping below 0.1 $\mu\text{S}/\text{cm}$ in less than two weeks. The faster reduction in water conductivity is in part due to

greater enforcement of cleanliness during the assembly of these systems. Measured water conductivity changes for both of these systems are summarized in Figure 3.17. A second regenerative heat exchanger was incorporated into systems #2 and #3 to further improve the heating performance of the test systems. In addition, an actively controlled water cooling system with an over temperature failsafe to shut down the heaters was incorporated into the third system to mitigate the relatively large swings in the temperature of the building-supplied water cooling loop and to deal with the possible failure of the building-supplied water cooling system. These improvements are being incorporated into the older systems as time permits.

Another shakedown test took place with the start of the first simulated PWR test. As with the first simulated BWR water tests, the test systems were first run at room temperature at the target water pressure to inspect for leaks. The systems were then slowly brought up to the target temperature. The process of creating, measuring, and controlling B and Li content in the water required systematic study. Water temperature uniformity was also measured during two PWR water shakedown tests. Thermocouples were placed at different locations along the length of the autoclave in each of the two tests with the resulting temperature profile shown in Figure 3.18. The temperature profiling also shows that the interior surface of the autoclave base plate operates at less than 260°C (500°F) while the omniseal operates at less than 230°C (446°F). (The maximum operating temperature of PTFE is approximately 300°C or 572°F.) Overall, the test systems are now working well and the day-to-day operation of the systems has taken on a more routine character.

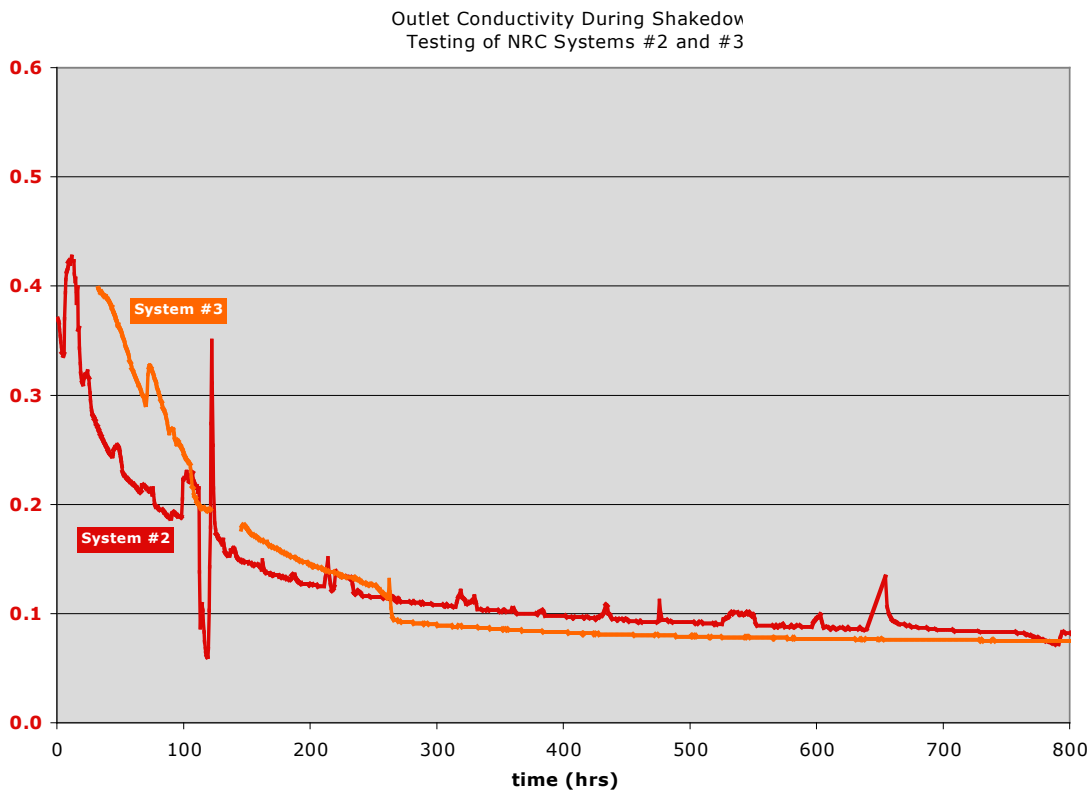


Figure 3-17 Outlet Water Conductivity as a Function of Test Time for Shakedown Tests in Systems #2 and #3

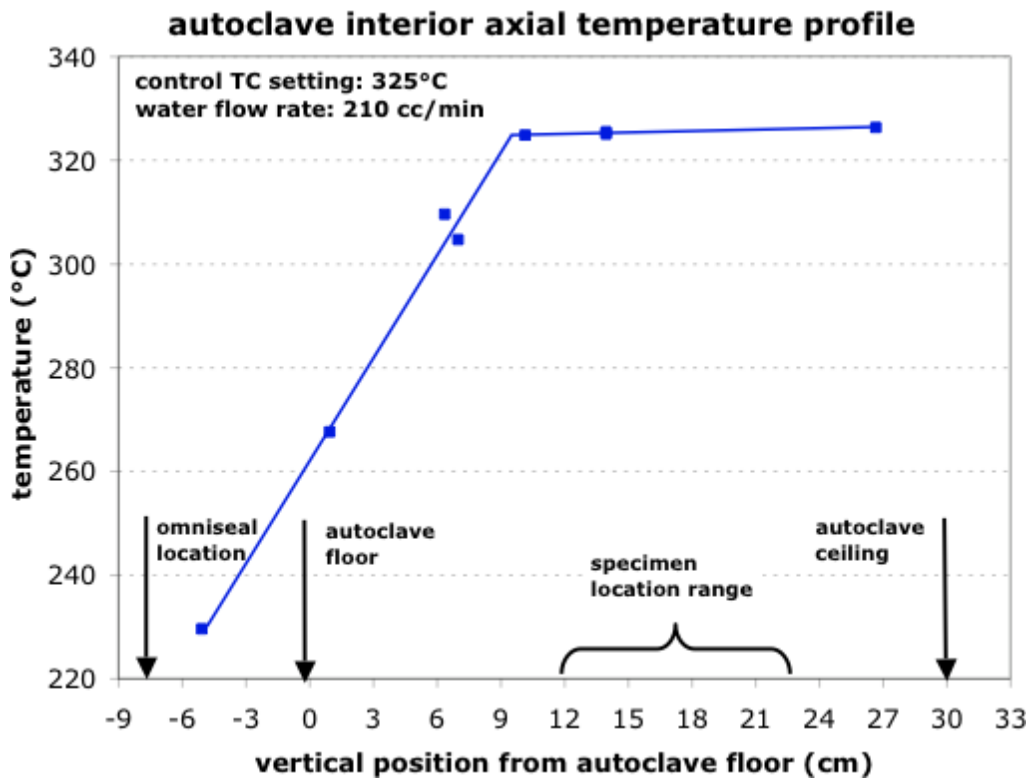


Figure 3-18 Autoclave Interior Axial Temperature Profile during a PWR Test at 325°C (617°F).